Supplementary Material

1. Supplementary figures S1 – S8
2. Supplementary tables ST1 – ST3

Roux-en-Y Gastric Bypass (RYGB) Surgery During High Liquid Sucrose Diet Leads to Gut Microbiota-Related Systematic Alterations

Laimdota Zizmare[1], Christina N. Boyle[2], Sabrina Buss[1], Sandrine Louis[3], Laura Kuebler[1], Ketki Mulay[4], Ralf Krüger[3], Lara Steinhauer[3], Isabelle Mack[5], Manuel Rodriguez Gomez[3], Kristina Herfert[1], Yvonne Ritze[4,*], Christoph Trautwein[1]

[1]Werner Siemens Imaging Center, Department of Preclinical Imaging and Radiopharmacy, Eberhard Karls University of Tübingen, University Hospital Tübingen, Röntgenweg 13, 72076, Tübingen, Germany;
[2] Institute of Veterinary Physiology, University of Zurich, Winterthurerstraße 260, CH-8057, Zurich, Switzerland;
[3] Department of Physiology and Biochemistry of Nutrition, Max Rubner-Institut, Haid-und-Neu-Straße 9, 76131, Karlsruhe, Germany;
[4] Department of Medical Psychology and Behavioral Neurobiology, Eberhard Karls University of Tübingen, Silcherstraße 5, 72076, Tübingen, Germany;
[5] Department of Psychosomatic Medicine and Psychotherapy, University Hospital Tübingen, Osianderstraße 5, 72076, Tübingen, Germany.
[*]Corresponding author: Yvonne Ritze, contact@yvonne-ritze.com

Supplementary Figure S1

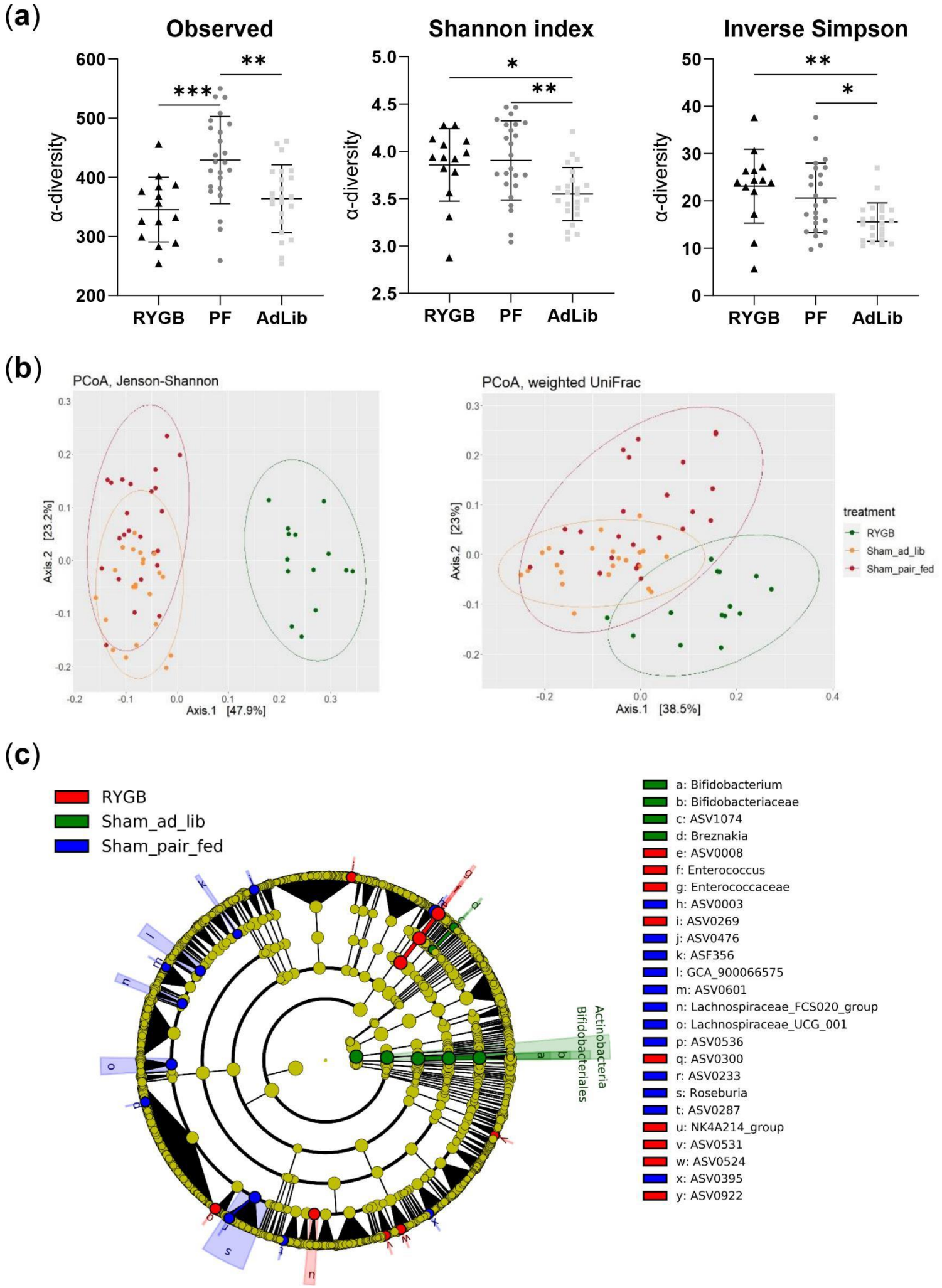

Supplementary Figure S1: Microbiota analysis. (**a**) α-diversity, the microbial community in AdLib animals was less diverse than in the other groups (diversity as the observed number of species, Shannon index and inverse Simpson). (**b**) β-diversity, principal coordinate analysis (PCoA) illustrating the separation of RYGB samples from the 2 other groups and showing the changes in the microbiota composition after surgery (PCoA based on either the Jenson-Shannon distance or the weighted UniFrac distance; each dot represents the whole gut microbiota from each animal at feces collection time). (**c**) LefSe analysis indicates the significant marker of each group represented in a phylogenetic cladogram. Pooled data was used from feces collection at four and eight weeks post-surgery, and at the day of euthanasia; *p*-values: *** < 0.001, ** < 0.01, * < 0.05.

Supplementary Figure S2

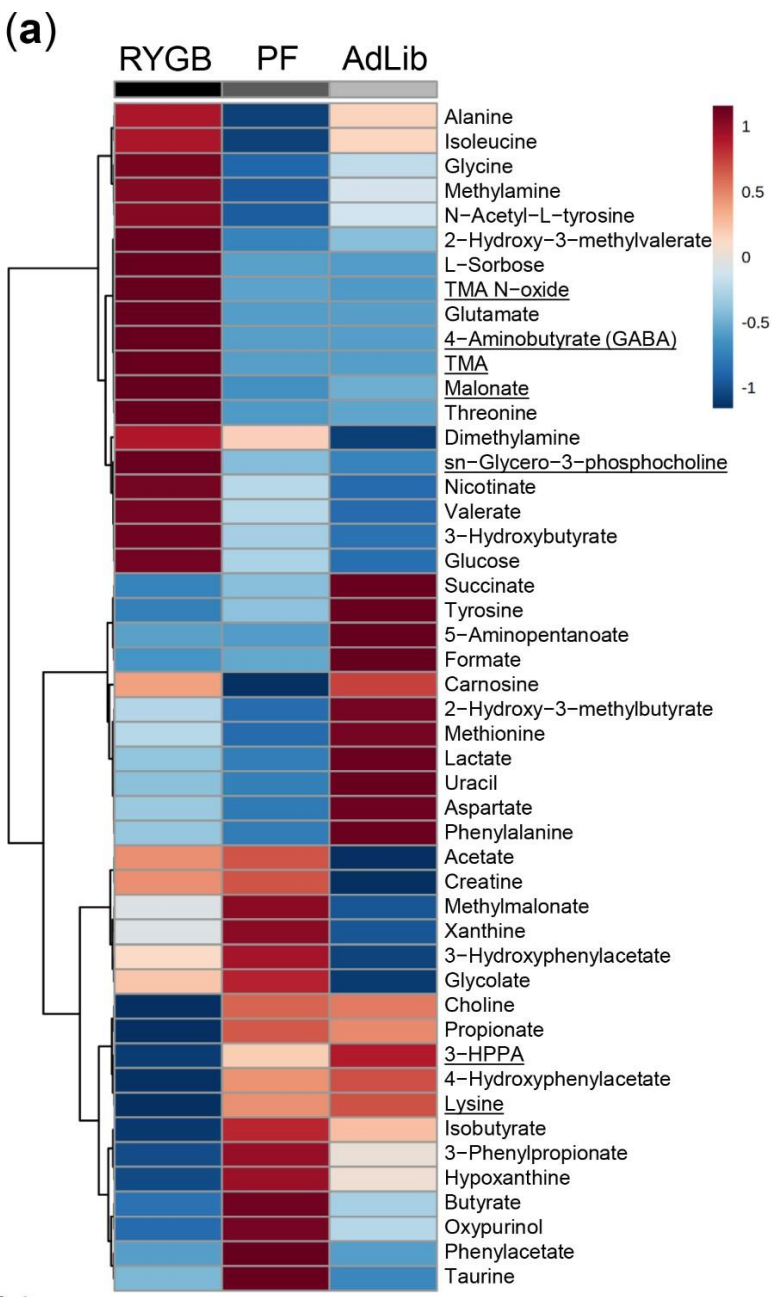

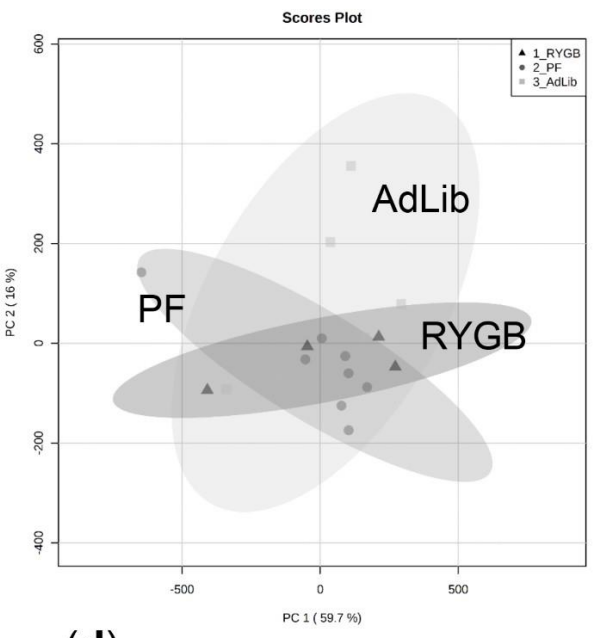

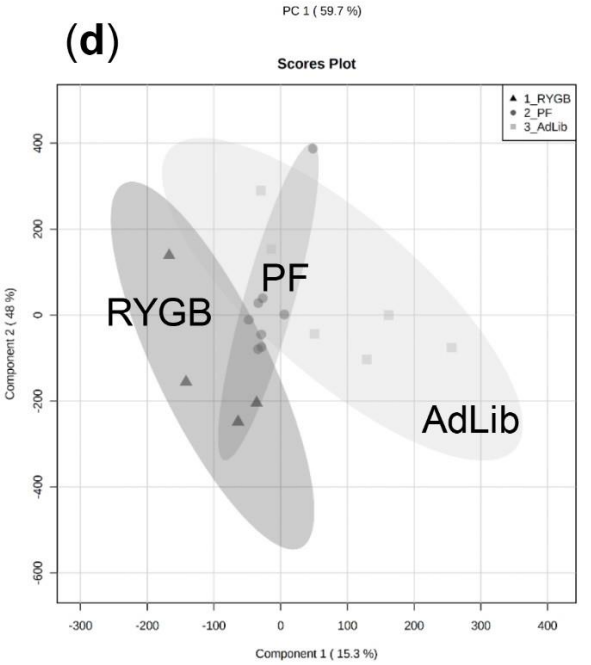

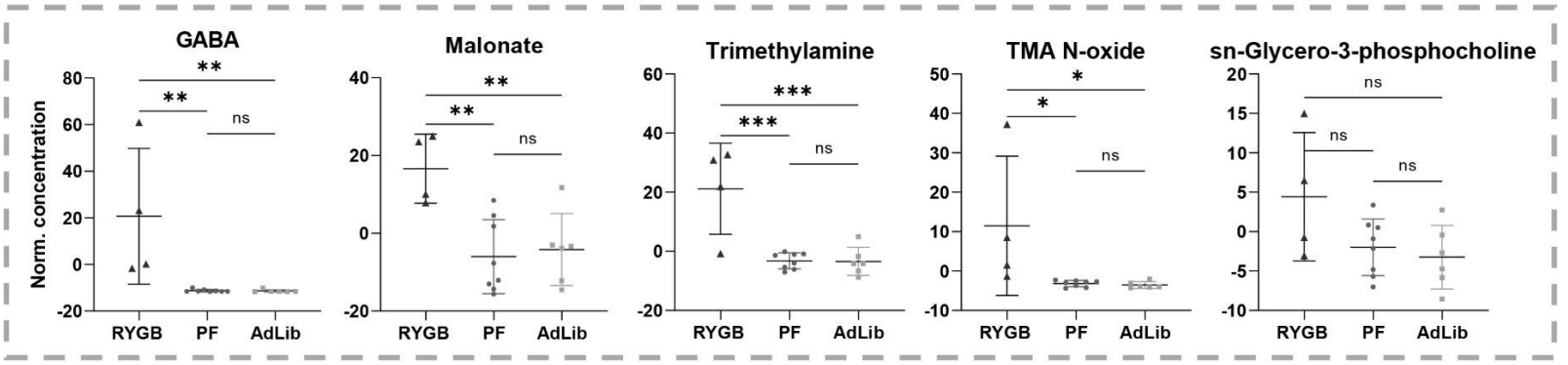

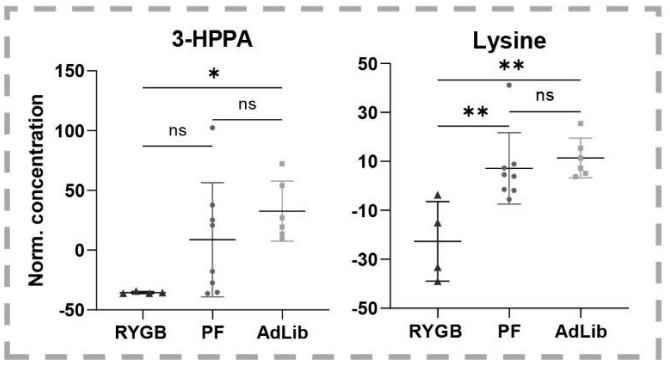

Supplementary Figure S2: Feces metabolomics four weeks after RYGB/sham surgery. (**a**) Averaged heat map illustrating all the quantified feces metabolites with their relative concentration increase (red) or decrease (blue). (**b**) Individual metabolite box plots. Decreased 3-hydroxyphenylpropionate (3-HPPA) and lysine in RYGB. Increased 4-aminobutyrate (GABA), malonate, trimethylamine (TMA) and TMA N-oxide in RYGB. Statistical significance based on one-way ANOVA with illustrated individual animal data points. (**c**) Principal component analysis (PCA) of feces samples 4 weeks after surgery. (**d**) Partial least squares discriminant analysis (PLSDA) regression model illustrating the further group cluster separation. 95% confidence regions are illustrated as clouds around the individual data points. RYGB (n = 4) (one animal excluded due to technical limitation of poor spectra resolution) black triangles, PF (n = 8) dark grey circles, AdLib (n = 6) light grey squares, *p*-values: *** < 0.001, ** < 0.01, * < 0.05.

Supplementary Figure S3

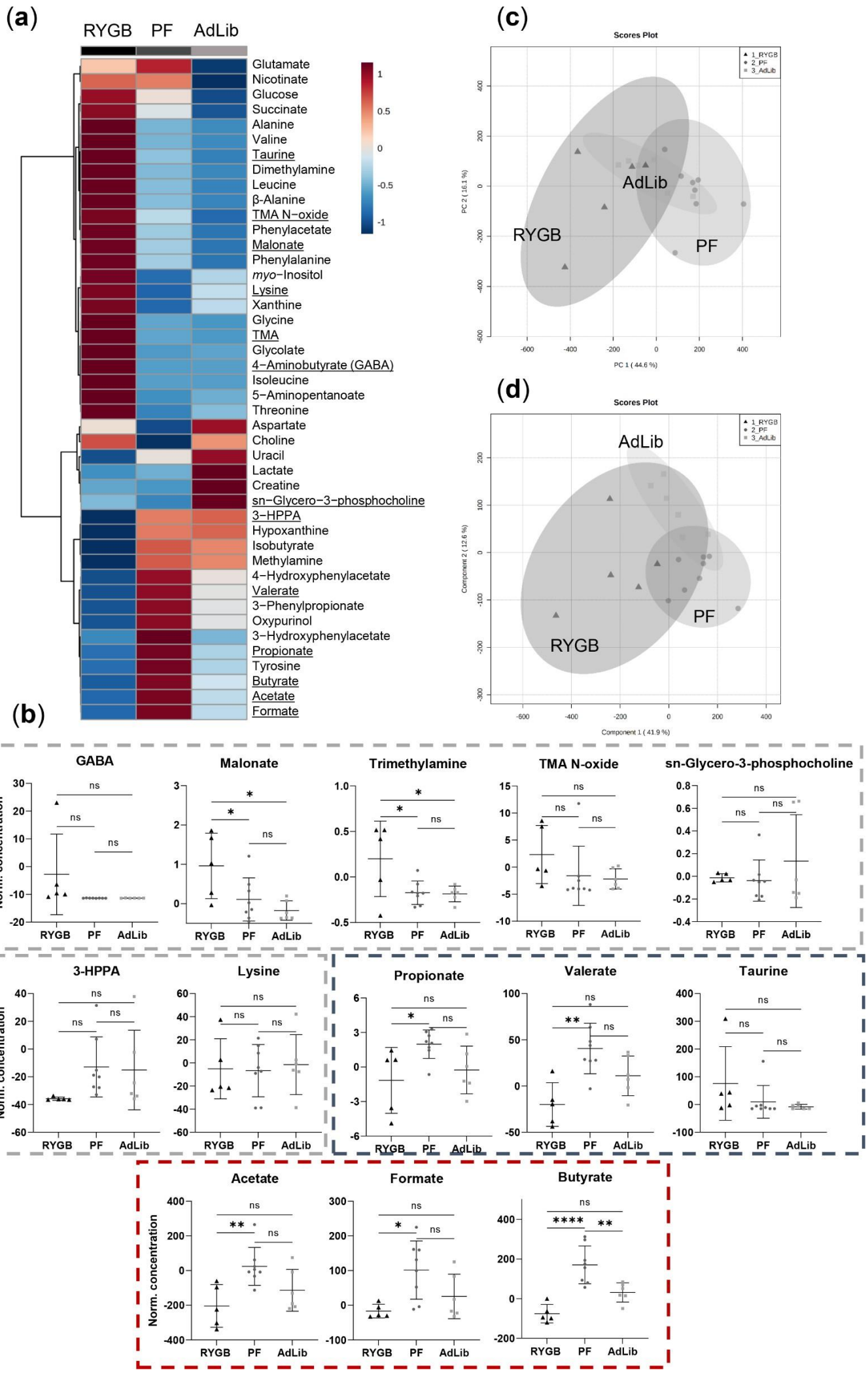

Supplementary Figure S3: Metabolite analysis of feces collected on the day of euthanasia from the colon after RYGB/sham surgery. (**a**) Averaged heat map illustrating all the quantified feces metabolites with their relative concentration increase (red) or decrease (blue). (**b**) Individual metabolite box plots. Grey box – feces metabolite patterns since week 4. Blue box – feces metabolite changes introduced at week 8. Red box – novel metabolite changes in feces collected on the day of euthanasia: decreased acetate, formate and butyrate in RYGB. Statistical significance based on one-way ANOVA with illustrated individual animal metabolite concentration as points. (**c**) Principal component analysis (PCA) of feces samples 4 weeks after surgery. (**d**) Partial least squares discriminant analysis (PLSDA) regression model illustrating the further group cluster separation with the RYGB sample sparsity. 95% confidence regions are illustrated as clouds around the individual data points. RYGB (n = 5) black triangles, PF (n = 8) dark grey dots, AdLib (n = 6) light grey squares, *p*-values: **** < 0.0001, ** < 0.01, * < 0.05.

Supplementary Figure S7

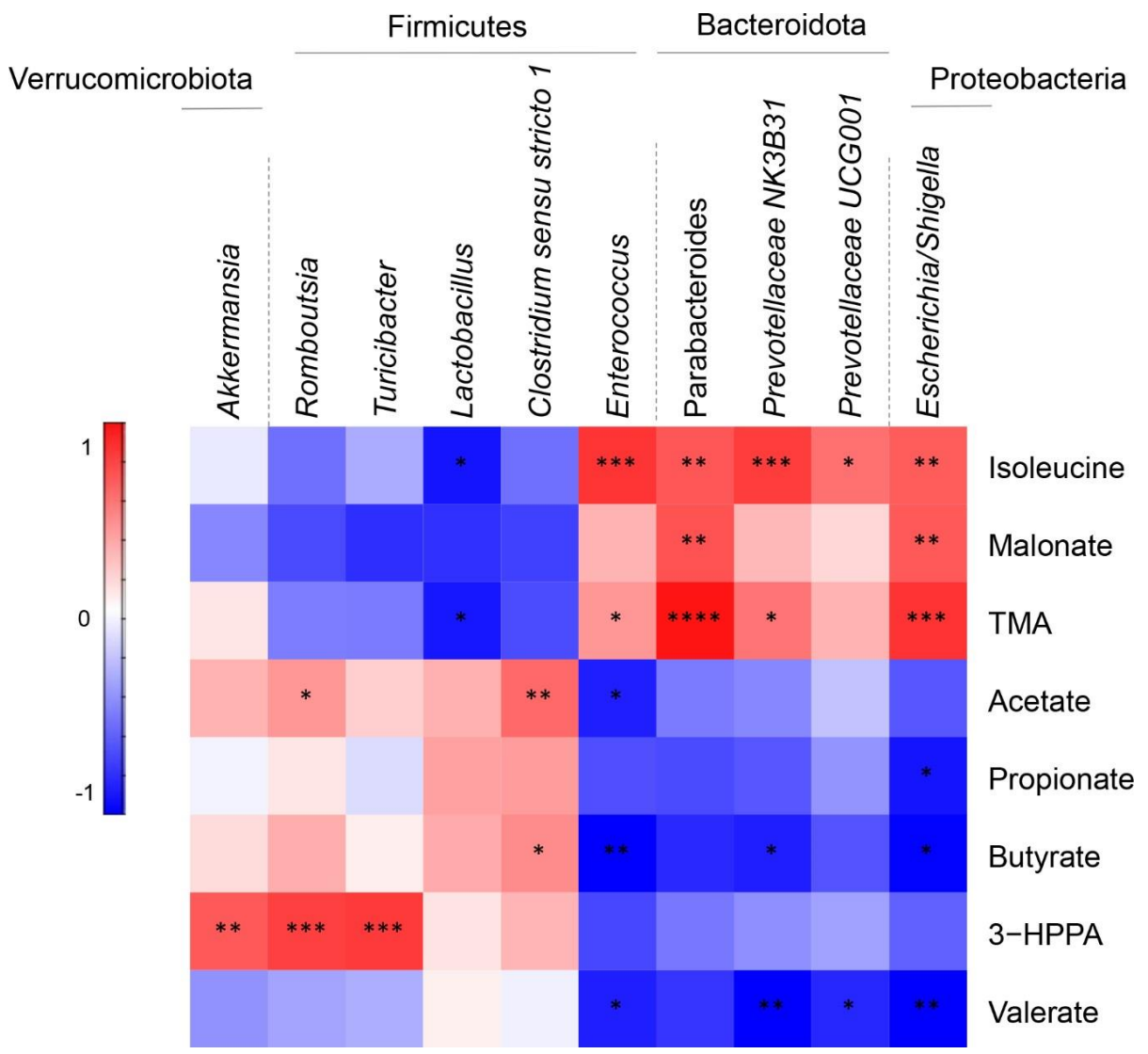

Supplementary Figure S4: Feces microbiota and metabolomics correlation analysis. Feces were collected directly from the colon on the day of euthanasia. 3-HPPA positively correlated with the relative abundance of *Turicibacter* and *Rombutsia*. TMA positively correlated with the relative abundance of *Escherichia/Shigella* and *Parabacteroides*. Isoleucine positively correlated with the relative abundance of *Prevotellaceae NK3B31* and *Enterococcus*. Color scheme illustrates the correlation values scaled between -1 and 1. Red color indicates a positive correlation, blue – negative correlation. Statistical significance of these correlations illustrated as *p*-values: **** < 0.0001, *** < 0.001, ** < 0.01, * < 0.05. Correlation analysis involves all three group (RYGB, PF and AdLib) feature values using Pearson r distance measure for the correlation coefficient determination.

Supplementary Figure S8

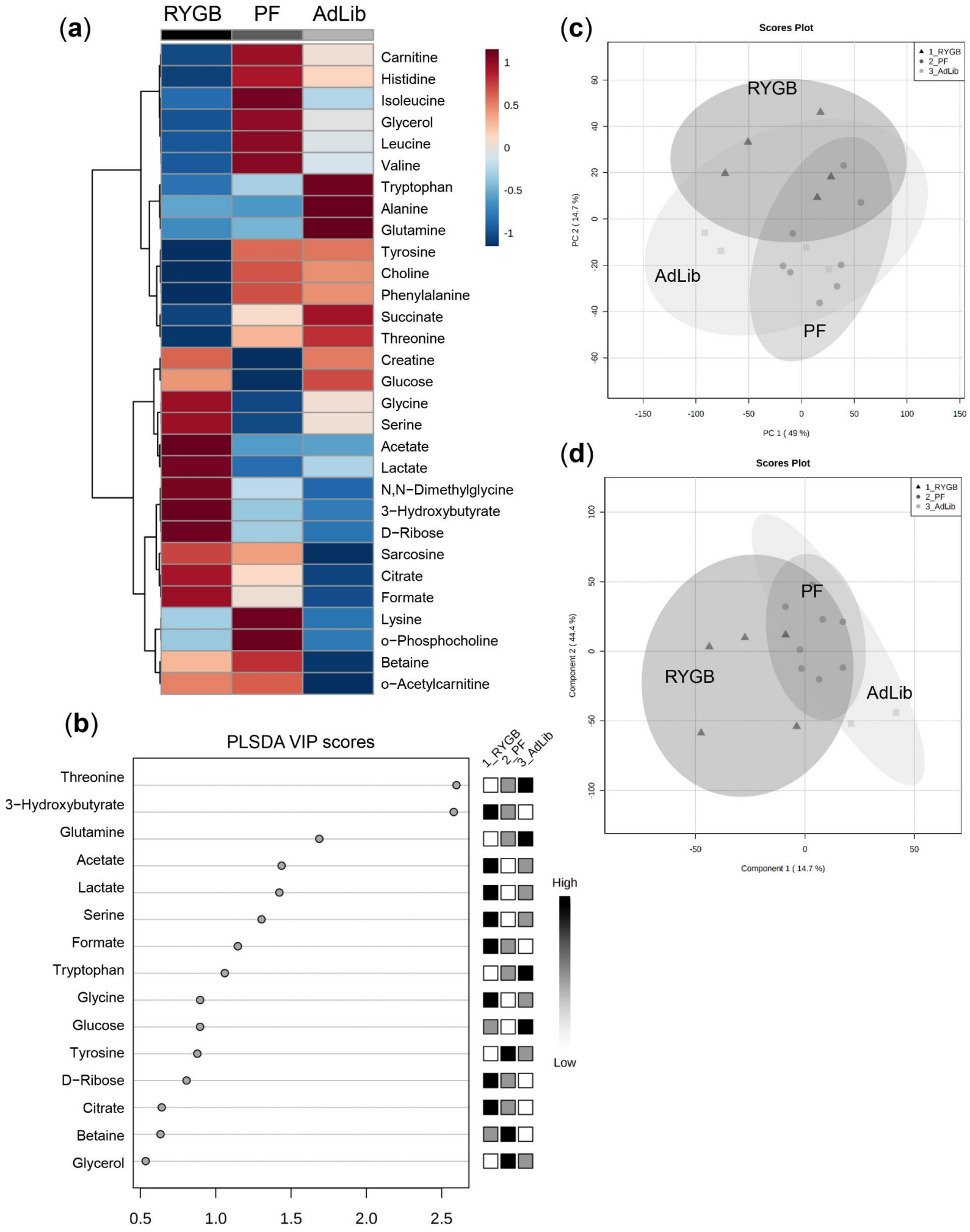

Supplementary Figure S5: Plasma metabolomics. (**a**) Averaged group metabolite concentration heat map illustrating all the quantified plasma metabolites with their relative concentration increase (red) or decrease (blue). (**b**) Partial least squares discriminant analysis (PLSDA) variable importance in projection (VIP) scores visualisation of most changing metabolites between the groups. (**c**) Principal component analysis (PCA) of plasma samples. (**d**) PLSDA regression model illustrating the further group cluster separation. 95% confidence regions are illustrated as clouds around the individual data points. RYGB (n = 5), PF (n = 8), AdLib (n = 6).

(a)

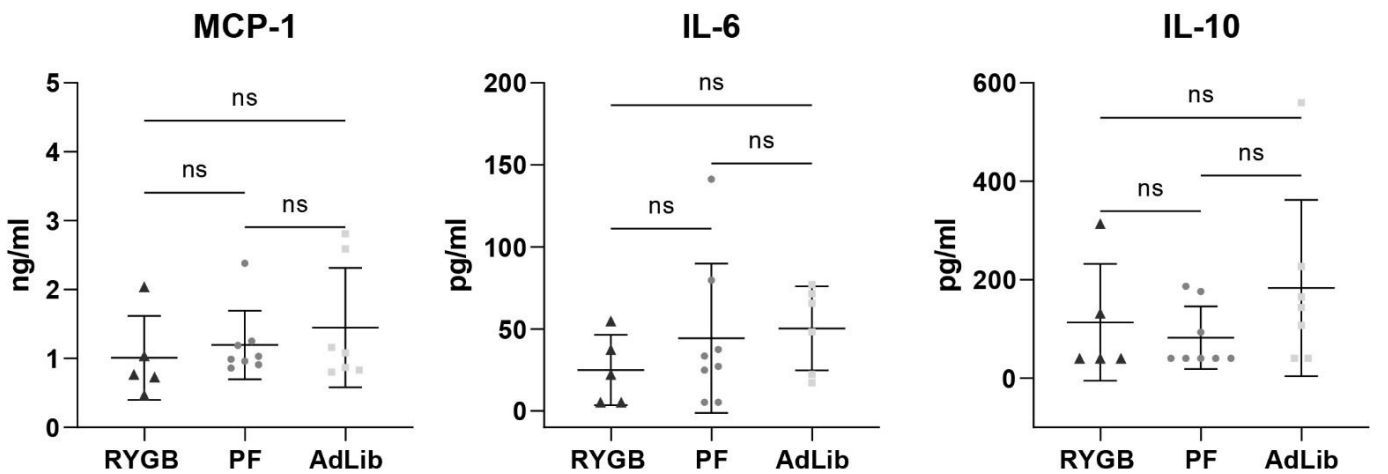

(b)

	RYGB	PF	AdLib
CXCL2 (pg/ml)	below LOD	below LOD	below LOD
IL-1α (pg/ml)	below LOD	below LOD	below LOD
IFN-γ (pg/ml)	below LOD	below LOD	below LOD
TNF-α (pg/ml)	below LOD	below LOD	below LOD

Supplementary Figure S6: Cytokine profiling of rat plasma. (**a**) Quantification of Monocyte Chemoattractant Protein-1 (MCP-1), Interleukin 6 (IL-6) and Interleukin 10 (IL-10), did not pass ordinary one-way ANOVA statistical significance threshold; (**b**) Chemokine ligand 2 (CXCL2), interleukin 1α (IL-1α), Interferon gamma (IFN-γ) and Tumour Necrosis Factor (TNF) were below the limit of detection (LOD). RYGB (n = 5) black triangles, PF (n = 8) dark grey dots, AdLib (n = 7) light grey squares.

Supplementary figure S7

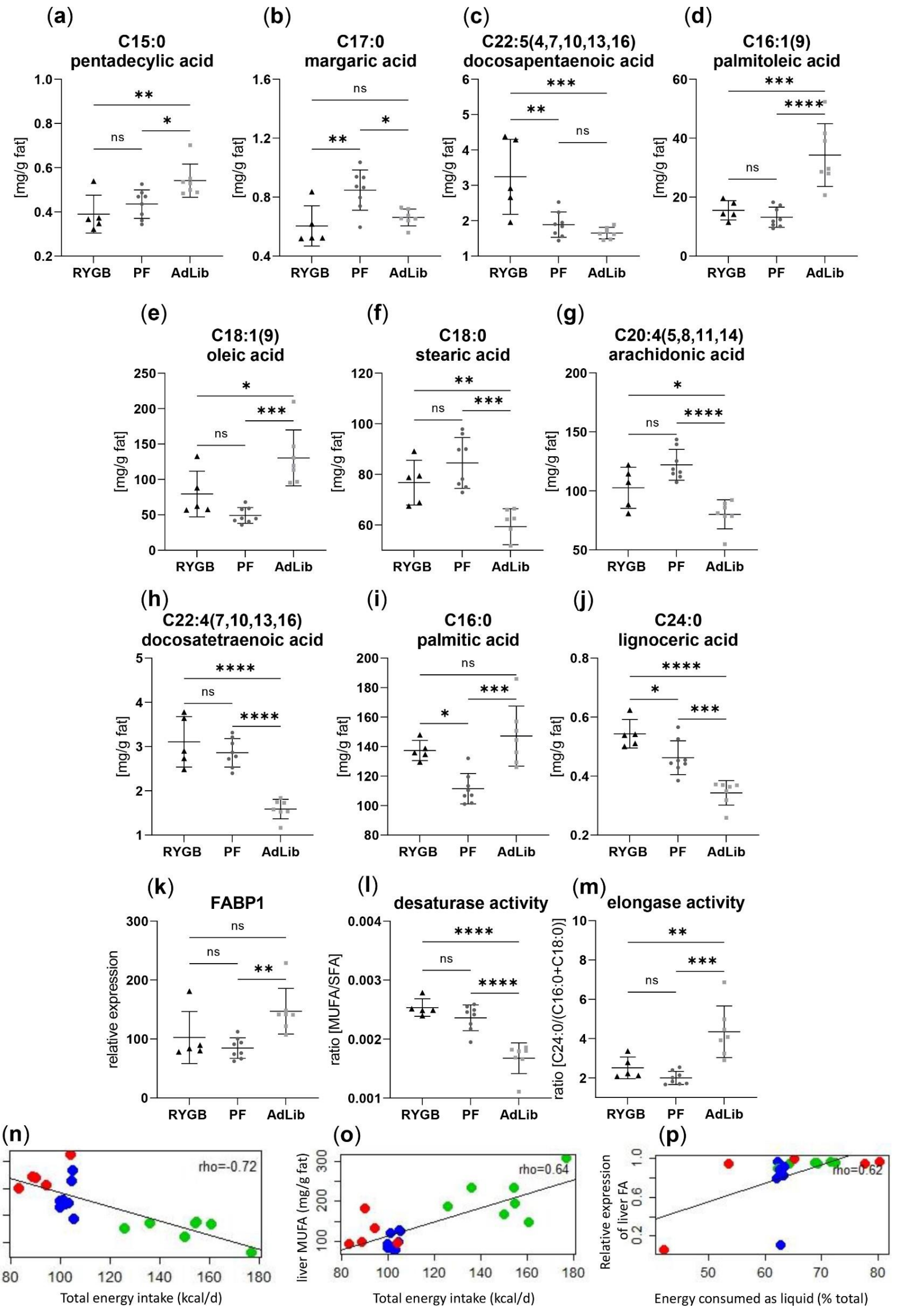

Supplementary Figure S7: Hepatic lipid analysis. Mass concentrations (mg/g fat) of hepatic lipid species upregulated in AdLib C14:0 (**a**), C15:0 (**b**), C16:1(9) (**c**), C18:1(9) (**d**); downregulated in AdLib C18:0 (**e**); C20:4(5,8,11,14) (**f**), C22:4(7,10,13,16) (**g**); downregulated in RYGB C18:1(11) (**h**); upregulated in RYGB C22:5(4,7,10,13,16) (**i**), C24:1(15) (**j**); downregulated in AdLib and slightly downregulated in PF C24:0 (**k**); upregulated in PF C17:0 (**l**); downregulated in RYGB C18:1(11) (**m**) compared to the other two groups. One-way ANOVA statistical significance test, RYGB (n = 5) black triangles, PF (n = 8) dark grey dots, AdLib (n = 7) light grey squares, *p*-values: **** < 0.0001, *** < 0.001, ** < 0.01, * < 0.05. (**n**) Correlations between the total energy intake (kcal/d) versus liver C24:0 (mg/g fat) (*p*=5.10-4; rho = -0.72) and (**o**) liver MUFA (mg/g fat) (*p*=0.0029; rho = 0.64); (**p**) correlation between the energy consumed as liquid (% total) versus relative expression of liver FAS (*p*= 0.0038; rho = 0.62). RYGB - red, PF - blue, AdLib - green.

Supplementary figure S8

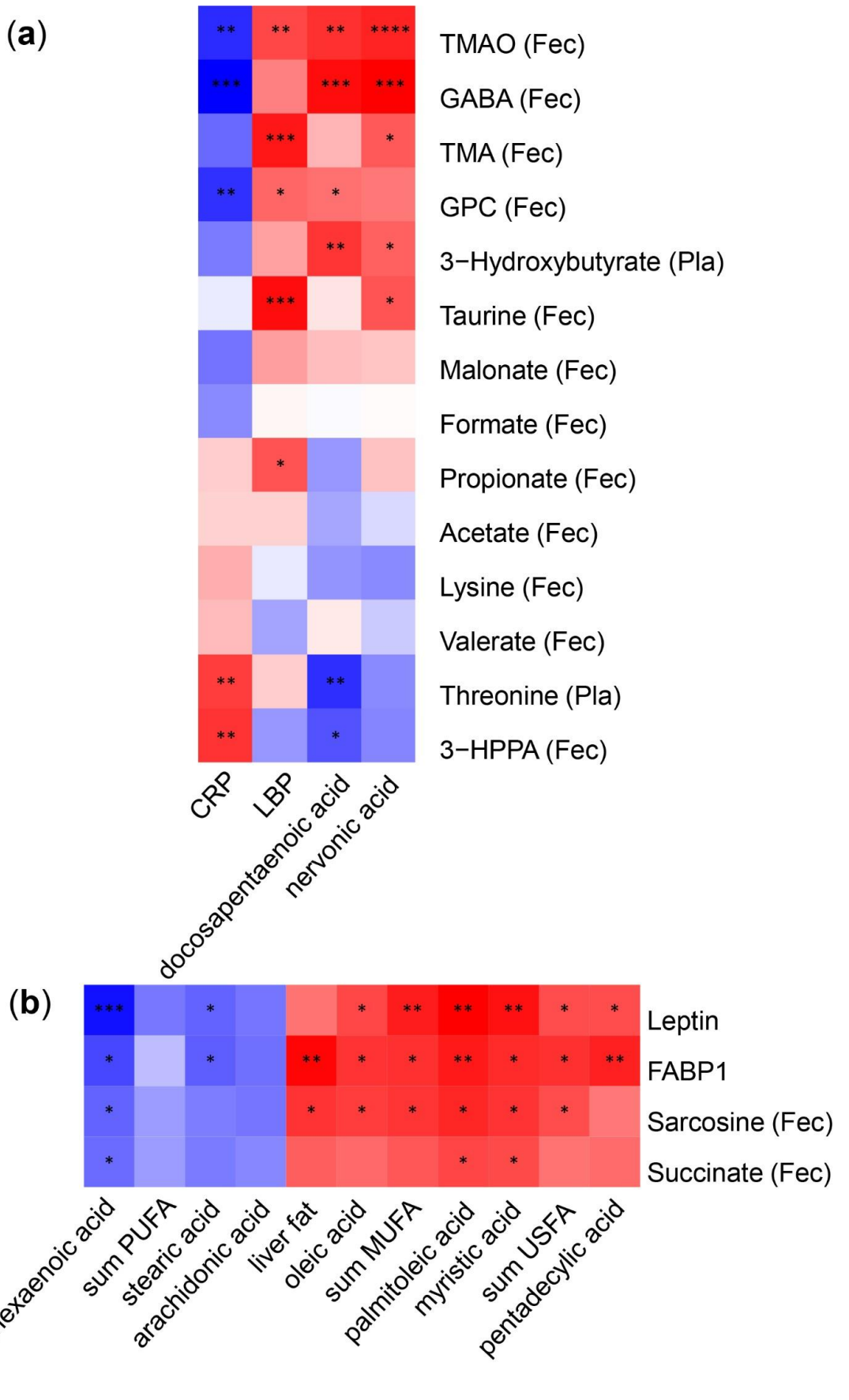

Supplementary Figure S8: Correlation maps of metabolites, immune, hormonal and liver parameters. (**a**) Sham vs. RYGB comparison significantly differing parameters, C22:5(4,7,10,13,16) (docosapentaenoic acid (osbond acid), PUFA, omega-6), C24:1(15) (nervonic acid, MUFA), (**b**) parameters similar between PF and RYGB (reduced food intake) compared to AdLib, C22:4(7,10,13,16) (docosatetraenoic acid, PUFA, omega-6), C16:1(9) (palmitoleic acid, MUFA), C14:0 (myristic acid, SFA), C15:0 (pentadecylic acid, SFA), C16:1(9) (palmitoleic acid, MUFA), *p*-values: **** < 0.0001, *** < 0.001, ** < 0.01, * < 0.05.

Supplementary Tables

Bregma -1.80		RYGB	PF	AdLib	*p*-value
PVH	Middle	3.00±1.66	8.43± 4.55	5.50±2.88	0.44
CeC	Right	7.33±2.63	2.80±1.01	3.40±1.68	0.16
	Left	10.87±4.60	4.27±1.10	5.47±3.81	0.32
DeN	Right	2.07±1.18	0.93±0.43	2.53±1.28	0.48
	Left	1.20±0.45	0.83±0.40	6.07±2.34	0.02*
BLA	Right	1.27±1.32	1.67±1.26	3.60 ± 1.82	0.44
	Left	0.87±0.60	4.40±3.68	2.87 ±2.45	0.57
layer 2 of cortex	Right	2.00±1.97	14.87±11.63	7.30±3.74	0.39
	Left	2.33±2.25	11.93±9.01	9.73±6.02	0.48

Supplementary Table ST1: Average number of c-Fos labelled cells in different brain areas after eight weeks of high sucrose diet in rats Average numbers were analyzed by counting cells on 3 distinct slices (60 µm thick) for every region. Data were analyzed by ANOVA test followed by a Tukey's post hoc test (p <0.05). Data are means ± SEM (n = 5). PVH – paraventricular hypothalamic nucleus; CeC – central amygdala; DeN – dorsal endopiriform nucleus; BLA – basolateral amygdaloid nucleus, anterior.

Bregma -1.80		RYGB	PF	AdLib	*p*-value
PVH	Middle	33.73±13.61	55.27± 22.14	35.07±10.10	0.51
CeC	Right	41.20±9.36	33.53±13.12	41.87±14.44	0.84
	Left	39.60±7.69	51.20±14.34	43.53±21.57	0.84
DeN	Right	123.40±23.86	124.53±24.11	91.93±19.55	0.26
	Left	122.87±25.44	159.30±7.05	132.67±32.02	0.48
BLA	Right	161.80±21.55	172.33±52.96	148.47±37.41	0.89
	Left	184.27±14.95	179.93±41.91	182.80±32.78	0.99
layer 2 of cortex	Right	338.67±27.05	314.77±38.82	339.20±37.31	0.82
	Left	318.53±17.72	372.63±30.71	263.13±59.22	0.14

Supplementary Table ST2: Average number of NeuN labeled cells in different brain areas after eight weeks of high sucrose diet in rats. Average numbers were analyzed by counting cells on 3 distinct slices (60 µm thick) for every region. Data were analyzed by ANOVA test followed by a Tukey's post hoc test if significant (*P<0.05; n.s., non-significant). Data are means ± SEM (n = 5). PVH – paraventricular hypothalamic nucleus; CeC – central amygdala; DeN – dorsal endopiriform nucleus; BLA – basolateral amygdaloid nucleus, anterior.

Bregma -1.80		Pair-fed	Ad-libitum	RYGB	p-value
PVH	Middle	4.47±2.74	2.93±1.78	2.10±1.25	0.65
CeC	Right	0.87±0.62	2.13±1.07	2.93±0.88	0.21
	Left	1.67±0.54	2.80±1.92	4.73±2.48	0.43
DeN	Right	0.93±0.43	1.13±0.83	0.73±0.38	0.86
	Left	0.60±0.36	3.87±2.05	0.40±0.30	0.08
BLA	Right	1.60 ±1.24	2.80±1.97	0.08±0.08	0.31
	Left	3.87±3.12	2.73±2.31	0.40±0.45	0.49
layer 2 of cortex	Right	14.60±11.57	4.33±3.48	2.00±1.97	0.36
	Left	11.60±8.73	7.13±6.38	2.27±2.27	0.53

Supplementary Table ST3: **Average number of co-localized cells (labeled by both c-Fos and NeuN) in different brain areas after eight weeks of high sucrose diet in rats.** Average numbers were analyzed by counting cells on 3 distinct slices (60 µm thick) for every region. Data were analyzed by ANOVA test followed by a Tukey's post hoc test. Data are means ± SEM (n = 5). PVH – paraventricular hypothalamic nucleus; CeC – central amygdala; DeN – dorsal endopiriform nucleus; BLA – basolateral amygdaloid nucleus, anterior.